CREATION OF A NOVEL FUSION PROTEIN WGA-ENPHR3.0 FOR CIRCUIT DISSECTION IN THE BRAIN

by

Lucas Kinsey

A Thesis
Submitted to the
Graduate Faculty
of
George Mason University
in Partial Fulfillment of
The Requirements for the Degree
of
Master of Science
Biology

Committee:

_____	Dr. Theodore Dumas, Thesis Chair
_____	Dr. Giorgio Ascoli, Committee Member
_____	Dr. Patrick Gillevet, Committee Member
_____	Dr. Iosif Vaisman, Director, School of Systems Biology
_____	Dr. Donna M. Fox, Associate Dean, Office of Student Affairs & Special Programs, College of Science
_____	Dr. Fernando R. Miralles-Wilhelm Dean, College of Science

Date: _____ Spring Semester 2023
George Mason University
Fairfax, VA

Creation of a Novel Fusion Protein WGA-eNpHR3.0 for Circuit Dissection in The Brain

A thesis submitted in partial fulfillment of the requirements for the degree of Master of Science at George Mason University

By

Lucas Kinsey
Bachelor of Science
George Mason University, 2020

Director: Theodore Dumas, PhD Program Director, Interdisciplinary Neuroscience Program
Associate Chair for Research
Interdisciplinary Neuroscience Program
Department of Psychology

Spring Semester 2023
George Mason University
Fairfax, VA

DEDICATION

To my beloved wife, Sarah.

ACKNOWLEDGEMENTS

I would like to thank my family for helping support my continued education, my trusted lab members Silanur Inanoglu. and Brandon Leon for motivating me and sharing in the work for the time we were working together. Thank you to the new undergraduates who were able to perform consistent electrophoresis gels that greatly benefited the data acquisition of this project. I would like to thank my advisor and mentor Dr. Theodore Dumas for not only offering good council, but also for helping reveal to me the direction I wanted my life to go in.

TABLE OF CONTENTS

LIST OF FIGURES

LIST OF ABBREVIATIONS

Adeno-associated viral vector ……	AAV
Alkaline Lysis ……	AL
Channelrhodopsin ……..	ChR
Endoplasmic Reticulum …….	ER
Entorhinal Cortex ……...	EC
Lauria-Bertani ……	LB
Halorhodopsin …….……..	eNpHR3.0
Parvalbumin-positive …….	PV+
Polymer Chain Reaction ……	PCR
Region of interest ……..	ROI
Super Optimal Broth with Catabolite Repression ……	SOC
Ultra-Chemically Competent Cells ……...	UCCs
Wheat Germ Agglutinin ……	WGA

ABSTRACT

CREATION OF A NOVEL FUSION PROTEIN WGA-ENPHR3.0 FOR CIRCUIT DISSECTION IN THE BRAIN

Lucas Kinsey

George Mason University, 2022

Thesis Director: Dr. Theodore Dumas

Over the last decade, optogenetic manipulation of neuronal activity has redefined functional circuit analysis in the central nervous system. Combined with promoters for specific neuron types, optogenetic actuators permit activation or inhibition of select neurons within intact circuits. A major advance in this field would be to enable movement across synapses to direct the optogenetic actuator to specific afferents of the target neuronal population. Fusion constructs of wheat germ agglutinin (WGA) have been shown to move retrogradely across synapses. In this thesis project, a transsynaptic optogenetic-construct was created by fusing WGA to the N-terminus of halorhodopsin (eNpHR3.0). This was done so by first amplifying the WGA sequence using mutagenic primers in a polymerase chain reaction (PCR) to flank the WGA fragment with restriction sites that match the insert location in eNpHR3.0. The PCR product was then ligated to the N-terminus of eNpHR3.0 and samples were transformed into E coli. Positive clones were verified to include the WGA sequence via restriction digest and electrophoresis. Positive plasmid samples were commercially sequenced in order to verify the WGA orientation. This novel WGA-eNpHR3.0 plasmid serves as a powerful tool to traffic eNpHR3.0 retrogradely both *in vivo* and *in vitro*.

INTRODUCTION

Background:

Optogenetic constructs allow for the analysis of neural circuits by modulating the activity of neurons exclusively with light. With the rapid development of the field over the past decade, there now exists a wide toolset of optogenetic actuators and indicators that allow for complex analysis of the brain (Kim et al., 2017). What makes optogenetics particularly compelling is the ability for these constructs to modulate genetically targetable neuronal cell types (Luo et al., 2008). This feature allows for precise control of neural circuits (De La Crompe et al., 2020). Such cell-specific stimulation experiments are essential to any neuroscientific question concerning causal relationships between brain regions, brain activity, and behavior (Jazayeri et al., 2017). Furthermore, some cited studies even argue precise optogenetic stimulation provides a more robust method of studying behavioral paradigms than electrophysiological microstimulation, such as being able to elicit certain aggressive behaviors in rodents that microstimulation techniques are not able to (Lin et al., 2011). This evidence suggests that it is a worthwhile endeavor to continuously improve these constructs to increase their specificity, such efforts may lead to discovery of novel neural mechanisms that drive cognitive states and complex behaviors in animals. The purpose of the proposed project is to modify an inhibitory optogenetic construct, halorhodopsin (eNpHR3.0) by fusing it to a retrograde trafficking protein called wheat germ agglutinin (WGA). With a history of WGA being capable of trafficking through retrograde synapses of infected neurons, the resulting WGA-eNpHR3.0 construct would enable the selective

inhibition of afferents to target neural populations, further refining the ability of this optogenetic tool to dissect central neural circuits (Damak et al, 2008, Baker et al, 1986).

There exists a large repertoire of optogenetic constructs that enable the optical interrogation of neural circuits. Some of the most broadly used optogenetic actuators are rhodopsin proteins (Guru et al., 2015). Rhodopsin proteins can be either excitatory, such as channelrhodopsins (ChR), inhibitory, such as halorhodopsins (NpHR), or they can even be engineered to achieve both excitation and inhibition depending on what wavelength of light that is used to stimulate them, such as recent variants of ChRs (Wietek et al., 2015). The appropriate use of each rhodopsin is dependent upon its ion selectivity (Mattis et al., 2011). ChR is characterized as a depolarizing rhodopsin; in its native state it is a blue light (450 nm) activated sodium channel. NpHR is characterized as a hyperpolarizing rhodopsin, where it acts as a yellow-light (588 nm) activated chloride pump. The development of each rhodopsin has involved the inclusion of mammalian codons and membrane localization signals to allow for more robust membrane expression, with one of the most recent developments on NpHR, adding a golgi trafficking sequence and endoplasmic reticulum (ER) export motif to prevent ER localization, and thus was subsequently named eNpHR3.0 (Gradinaru et al., 2010). In applications where neuronal inhibition is required, eNpHR3.0 has beneficial applications as well as potential limitations. As stated, eNpHR3.0 is a yellow-light activated chloride pump, the benefit of using eNpHR3.0 is that it possesses one of the most red-shifted excitation spectrums out of the other inhibitory optogenetic constructs in its class which permits photostimulation in deeper tissues (Ash et al, 2017). However, one limitation of this construct is the intracellular accumulation of chloride it generates upon prolonged activation. This can alter the effect of GABA receptor currents and as the intracellular chloride concentration is raised passed the critical concentration

that sets the reversal potential for chloride (Wiegert et al., 2017, Raimondo et al., 2012). Despite these drawbacks, halorhodopsin possesses the unique ability to pump chloride inside of the cell against the concentration gradient of chloride, making halorhodopsin an attractive protein for optogenetic inhibition of neurons.

Optogenetics used in conjunction with neuronal tracing strategies have produced tools to also enable targeted stimulation of specific neuronal circuits (Grosenick et al., 2015). Optimized strategies for circuit dissection involve the trafficking of constructs across synapses, either through viral vectors or with specific protein constructs. Most strategies that use viral vectors for genetically modifying neurons to express optogenetic constructs involve the use of adeno-associated viral vectors (AAV). AAV viruses are the most efficient vector for optogenetic applications due to the low toxicity in developed serotypes and efficient expression of transgenic proteins (McCarty et al., 2001, Kwon and Schaffer, 2008). Additional functional modifications have been included in AAV vectors such as AAV-retro, a virus that allows for transfection of projection neurons for efficient dissection of neural circuits when combined with optogenetic tools (Tervo et al., 2016). Other approaches also exist to trace connectivity back to projection neurons using transsynaptic trafficking viruses. For instance, a glycoprotein deleted rabies virus will traffic retrogradely to monosynaptic afferents if the presynaptic neuron has been transfected with a rabies compatible envelope protein (Wickersham et al., 2007). An alternative to using a viral vector for neuronal retrograde tracing would be to use a particular protein that has transsynaptic retrograde trafficking qualities, such as wheat germ agglutinin (WGA). WGA can be observed in distant cerebellar granule cells when expressed in Purkinje cells (Yoshihara et al. 1999) and in the nucleus of the diagonal band of OMP-WGA mice when expressed in the olfactory bulb, indicating retrograde trafficking activity (Shipley et al., 1995). It is theorized that

this mechanism involves a 27 amino acid signal sequence that packages the protein into vacuoles, allowing for inclusion into dendritic endosomal secretory systems for exocytosis (Yoshihara et al., 1999, Broadwell and Balin, 1985). WGA was recently shown to be non-toxic *in vivo* when used to demonstrate retrograde trafficking of the DNA recombinase, Cre, between neurons within adjacent ipsilateral cortical regions or across hemispheres from one hippocampus to the other (Gradinaru et al., 2010). Furthermore, WGA has been successfully demonstrated as a first order and second order retrograde tracer of neurons that innervate taste cells (Damak et al., 2008). Thus, WGA offers a promising tool for retrograde transsynaptic neuronal trafficking of optogenetic constructs for genetic dissection of neural circuits anywhere in the brain.

This project will create a retrograde transsynaptic halorhodopsin viral vector by fusing WGA to eNpHR3.0 in an adeno-associated viral vector (AAV). AAV enables transgene delivery of the construct to the desired target. Post-transcription in the target neurons, the WGA→eNpHR3.0 mRNA will be translated in the endoplasmic reticulum (ER) and trafficking sequences located within the construct itself direct the protein to the plasma membrane (Gradinaru et al., 2010). Secretory sequences located in WGA then permit exocytosis from postsynaptic neurons and endocytosis by associated presynaptic terminals (Broadwell and Balin, 1985, Yoshihara et al., 1999). Following uptake of this fusion construct, we hypothesize that the protein will be further trafficked to the neuronal soma, where it will then be repackaged in the endosome and trafficked to the cellular membrane of the neuron due to the Golgi and ER export motifs included in eNpHR3.0.

Immediate Purpose:

In its current form, the product of this project, WGA-eNpHR3.0-EYFP, will enable the optogenetic silencing of afferent neurons to Cre-positive target neurons. The dorsal hippocampus and its associate with spatial learning and memory serves as an attractive model to test our new construct. The hippocampus contains neurons tuned to specific locations in space, termed "place cells," which are believed to permit the animal to understand its location in a geometric space that has been coded upstream in the entorhinal cortex (O'Keefe and Dostrovosky, 1970, Deshmukh et al., 2010). The coordination of place cell discharge in the hippocampus has been linked to theta (4-12 Hz) and gamma (25-140 Hz) oscillations along with sharp wave ripples (SWRs, 120-200 Hz) that can be observed in local field potentials recorded in area CA1 (Buzsáki, 2015, Colgin, 2016). Spatial information encoding and retrieval appear to be separately coordinated by different subsets of these oscillations (Senior et al., 2008, Headley and Paré, 2017). Theta power has been linked to spatial exploration, increases during animal movement, and is a function of running speed. Spatial information encoding, updating, and retrieval are thought to occur at different phases of each theta cycle (Hasselmo and Stern, 2014) enabling theta oscillations to coordinate the sequential activity of ensembles of hippocampal pyramidal neurons that guide the animal's trajectory during movement towards a goal (Johnson and Redish, 2007, Diba and Buzsáki, 2007; Cabral et al., 2014). Theta phase also modulates the power of gamma oscillations, though this interaction is only partially understood (Belluscio et al., 2012).

Gamma oscillations have been subdivided into slow (25-55 Hz) and fast gamma bands (60-120 Hz) (Colgin, 2016). Slow gamma in hippocampal area CA1 is thought to be involved in memory retrieval (Steffenach et al., 2002; Colgin and Moser, 2010) and has been shown to arise

from input activity entering from area CA3 pyramidal neurons that synapse onto parvalbumin positive (PV+) basket cells in area CA1. In contrast, fast gamma power may reflect ongoing processing of spatial information (Brun et al., 2002; Fyhn et al., 2004; Hafting et al., 2005) and is regulated by inputs from the entorhinal cortex (EC, layer III)(Colgin et al., 2009; Colgin and Moser 2010) and also synapse onto PV+ basket cells in area CA1. Thus, these PV+ basket cell interneurons appear to be the focal point for the regulation of slow and fast gamma. An increase in slow gamma power occurs during animal immobility, and the activity of neuronal ensembles during SWRs that code for future movement to a remembered location occur across slow gamma cycles (Pfeiffer and Foster, 2015; Zheng et al, 2016). During epochs of increased fast gamma power, sequences of pyramidal cell discharge more closely track the position of the animal and occur within each gamma cycle (Zheng et al, 2016). Overall, these data support the notion that activation states in area CA1 (slow versus fast gamma) are driven by separate inputs onto the same internal architectures (PV+ basket cells) and that these activation states reflect the cognitive state of the animal, either updating current location or projecting future movement trajectory. While anatomical and physiological data indirectly support these notions, it has yet to be demonstrated directly that PV+ interneurons regulate the generation of both slow and fast gamma. Moreover, causal links between CA3 and EC afferents to PV+ interneurons and slow and fast gamma oscillations have not been established.

Confirmation or refutation of these postulates will be made possible by our new WGA-eNpHR3.0 construct. In the AAV vector backbone, eNpHR3.0-EYFP sits in a 3’ to 5’ orientation between pairs of lox sites. WGA will be inserted on the 5’ side of eNpHR3.0 within the lox pairs. In the presence of Cre-recombinase, the sequence between the lox sites is inverted and WGA-eNpHR3.0-EYFP will be expressed. As such, when this construct is incorporated into viral

particles and injected into area CA1 of PV-Cre mice, it will be expressed in these basket cells and transported retrogradely to the CA3 and EC afferents enabling target specific silencing of either or both inputs. More broadly, this transsynaptic optogenetic technology has the potential applications in numerous brain regions, in various organisms, and organic and synthetic tissue preparations.

METHODS

Acquiring and Preparing Plasmid Stock:

Two plasmids were used to create the fusion protein construct WGA-eNpHR3.0-EYFP, both ordered from AddGene. The plasmid containing eNpHR3.0-EYFP was pAAV-DIO-EF1α eNpHR3.0-EYFP (Gradinaru et al. 2010), while the plasmid containing WGA was pAAV-THP-GFP/WGA. Both plasmids were received in the form of a bacterial stab from which they were simultaneously grown for 16 hours in Luria-Bertani (LB) broth (shaking at 37°C). Serial dilutions of 1:10, 1:100, and 1:000 for each plasmid culture were then prepared and 100 µL of each dilution was plated on LB agar containing ampicillin (20 µg/mL). Plates were then incubated overnight at 37°C.

Isolating DNA:

Plasmid DNA was purified from bacterial cultures through alkaline lysis (AL) miniprep. Cells were pelleted through centrifugation for 5 minutes containing RNase A, and then lysed with sodium hydroxide/sodium dodecyl sulfate (pH 8.0). A potassium acetate/acetic acid neutralization buffer was added to precipitate out the cell membrane, proteins, and genomic DNA (pH 4.7). The samples were centrifuged (14,000 RPM at 4°C) and the supernatant was kept. Two and a half volumes of 100% isopropanol were added, and the tubes were chilled at -80°C for 15 minutes prior to centrifugation for 10 minutes (14,000 RPM at 4°C). The supernatant was discarded, and DNA pellets were washed with 70% ethanol at room temperature and centrifuged for 5 minutes (14,000 RPM at room temperature). The 70% ethanol was aspirated, and pellets were allowed to

dry on the bench for at least 30 minutes. After ethanol evaporated, DNA pellets were resuspended in RNase-free sterile dH20. Concentration of the DNA was measured via a spectrophotometer and quality was tested via agarose gel electrophoresis.

Confirming Plasmid Identity:

Diagnosis of each plasmid was performed via restriction enzyme digestion (restriction enzyme, buffer, and plasmid incubated at 37°C for one hour). Enzymes EcoRI and BsrGI each cut the WGA plasmid and the NpHR3.0 plasmid once. For the WGA plasmid, EcoRI cuts at 2660 bp, while BsrGI cuts at 3395 bp. For eNpHR3.0 plasmid, EcoRI cuts at 3379 bp and BsrGI cuts at 1595 bp. Single digests with either enzyme produce full length linearized plasmids for the WGA plasmid (7322 bp total length) and the NpHR3.0 plasmid (7276 bp full length). Double digests with both enzymes produce bands at 6587 bp and 735 bp for WGA and 5492 bp and 1748 bp for eNpHR3.0.

PCR Amplification of WGA gene with Mutagenic Primers:

The WGA sequence was amplified from the WGA plasmid with a PCR reaction that contained mutagenic primers. A diagram is illustrated in Figure 1. A unique NheI restriction site at the end of the amino terminus of eNpHR3.0 and within the lox sites served as the insertion site for WGA. NheI sequences were included in both forward and reverse primers along with an extra platform base pair for better DNA polymerase annealing. The following primers produced single bands at the predicted length:

Forward – 5’-GGCTAGCTCCGGCCGGACTC-3’ (annealing temp = 71.7 °C)

Reverse – 5’CGCTAGCTTAAGCGTCACAGCCGCC-3’ (annealing temp = 73.9 °C)

The underlined portions indicate the NheI sequences and the base pair to include the 5’ side of the restriction enzyme sequence served as the platform. DreamTaq DNA Polymerase (Invitrogen) was used in this PCR reaction because of its low error rate (2.2e-5 errors per nucleotide per cycle). PCR products were diagnosed by gel electrophoresis and only reactions that showed a single band at the predicted length were used for ligation.

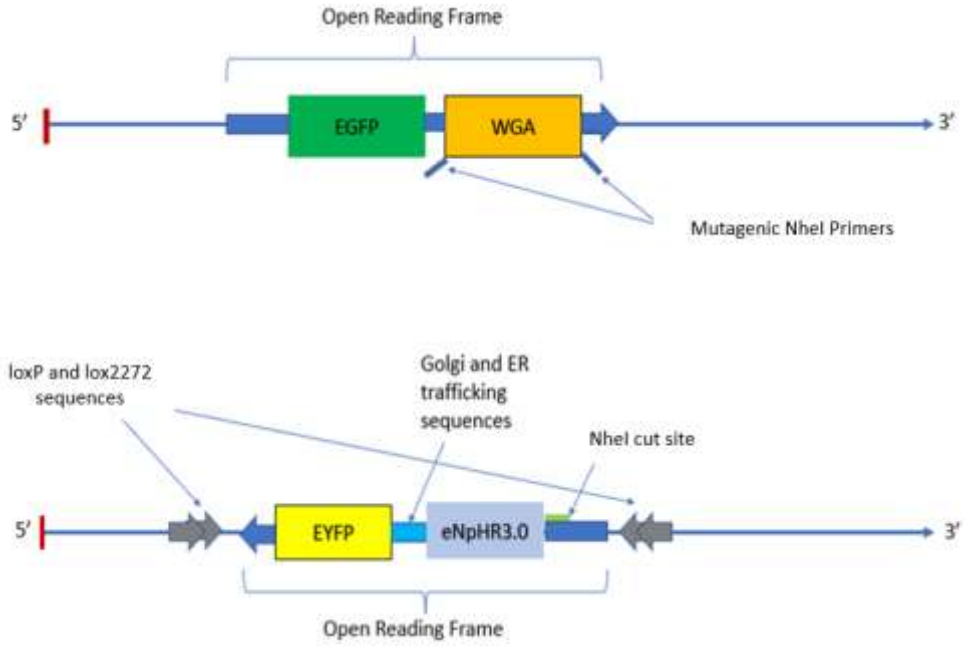

Figure 1. Conceptual Diagram of a Mutagenic PCR Reaction. On top, a symbolic representation of a linearized wheat germ agglutinin plasmid is demonstrated with the approximate placement of the WGA gene with mutagenic primers placed on each flank. Below, a symbolic representation of a linearized halorhodopsin plasmid is depicted with eNpHR3.0-EYFP orientated 3’ go 5’ between double lox sites (enabling inversion in the presence of Cre recombinase). A unique NheI restriction site at the N-terminus of eNpHR3.0 serves as the insertion site for WGA (green bar).

Ligation of WGA into eNpHR3.0 Plasmid:

Two preparations of WGA PCR product were prepared for ligation into eNpHR3.0 plasmid. The first WGA PCR product along with the eNpHR3.0 plasmid were digested with NheI (in CutSmart buffer at 37°C) for one hour followed by addition of another 0.5 µL of NheI and another hour of incubation to optimize the digestion. Digest products from this preparation were isolated by phenol:chloroform:isoamyl alcohol extraction and purified by ethanol extraction. For ligation, the vector (NpHR3.0) and insert (WGA) were mixed at molar ratios of 1:3, 1:6, and 1:12 and incubated in T4 DNA ligate and reaction buffer (Invitrogen). The second preparation involved a blunting reaction that uses a DNA Polymerase I, Large Klenow Fragment (New England Biolabs) to remove the 5' overhang on the NheI cut site in the eNpHR3.0 plasmid. For this reaction, purified eNpHR3.0 plasmid was digested with NheI (in CutSmart buffer at 37°C) before it was dissolved in T4 DNA Ligase Reaction buffer supplemented with 33 µM of each dNTP. A Klenow DNA Polymerase was then added to the DNA and the mixture was incubated on a tabletop for 15 minutes (25°C). For ligation, vector (NpHR3.0) and insert (WGA) were mixed at molar ratios of 1:3, 1:6, and 1:12 and incubated in a T4 DNA Ligate (Invitrogen).

Transformation of WGA->eNpHR3.0 plasmid into E. Coli:

The ligation reaction products were transformed into Stbl3 ultra chemically competent E. Coli cells (UCCs) (New England Biolabs) by adding 5 µL of the ligation reaction to 50 µL of the UCCs as soon as they thawed on ice and mixing well with the pipette tip used for the column transfer. The cells and the plasmid were allowed to incubate on ice for 30 minutes to allow the plasmid to attach to the UCC's outer membrane before a brief heat shock at 42°C for 45 seconds to induce uptake of the plasmid into the UCCs. The UCCs were immediately returned to ice for 5 minutes followed by addition of glucose enriched Super Optimal Broth with Catabolite

Repression (SOC Broth – 250 µL) and then incubated in a shaker at 225 RPM at 37°C for once hour. Transformed UCCs were plated on ampicillin (20 µg/mL) agar plates for ampicillin selection. Plates were then allowed to incubate overnight at 37°C.

Isolation and Identification of the WGA-eNpHR3.0 Fusion Construct:

Colonies were selected at random and incubated in 3 mL LB broth with 3 µL of 20 µg/mL ampicillin for 16 hours at 37°C and shaking at 225 RPM. Plasmid was purified from these cultures by alkaline lysis miniprep and then diagnosed by restriction digest to identify plasmids with inserts. NheI digests liberated the WGA insert. The ligation reaction produced at least 2 plasmid variants because the same restriction site exists on both ends of the WGA insert. Thus, when ligated into the eNpHR3.0 vector, WGA can be inserted 5'->3' or 3'->5'. In order to distinguish plasmids containing separate orientations of the WGA fragment, plasmids with inserts underwent DNA sequencing (GeneScript). Sequencing results will be used to verify the location and direction of the insert.

RESULTS

Halorhodopsin and wheat germ agglutinin plasmids were obtained from AddGene. We chose to work with the enhanced halorhodopsin, eNpHR3.0, which was contained in the plasmid pAAV-Ef1α-DIO eNpHR3.0-EYFP. WGA fragments were amplified from the plasmid pAAV2.5-THP-GFP/WGA. Plasmid maps are illustrated in Figures 2 and 3 below.

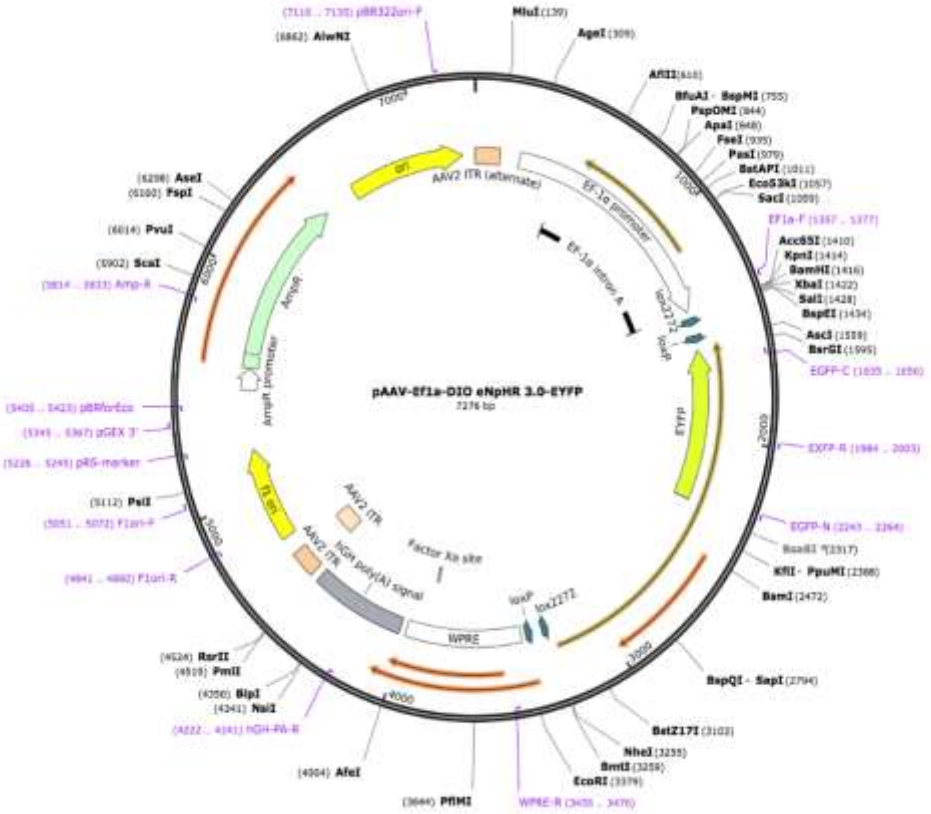

Figure 2. The plasmid map for pAAV-Ef1α-DIO eNpHR3.0-EYFP (7276 bp).

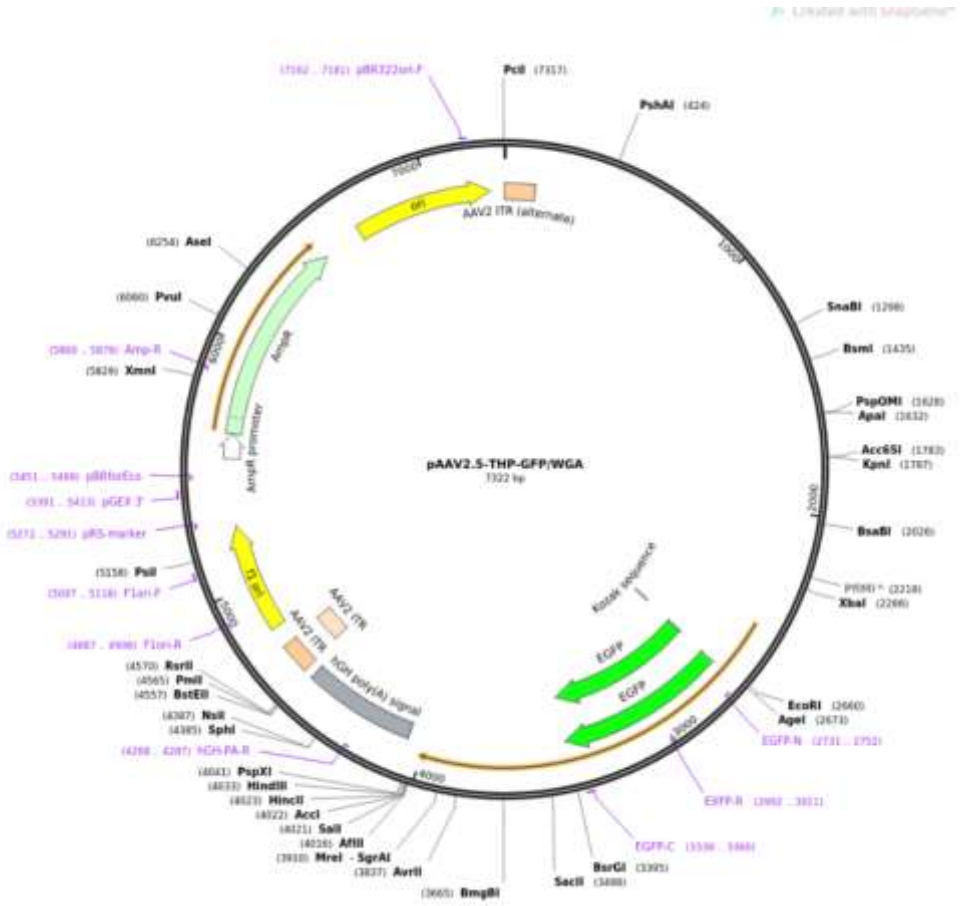

Figure 3. The plasmid map for pAAV2.5-THP-GFP/WGA (7322 bp).

Both plasmids were transformed into ultra-chemically competent E. Coli (pAAV-EF1α-DIO eNpHR3.0-EYFP into Stbl3 cells; pAAV2.5-THP-GFP/WGA into DH5α cells) and plated on Luria Bertani agar with ampicillin (20 µg/mL). Amplified plasmids were extracted from the cultures via an alkaline lysis miniprep procedure that included RNase A (10 µg/mL)in the resuspension buffer to remove bacterial RNA. Gel electrophoresis was used to verify plasmid quality (Figure 4) and concentration was determined via UV spectrophotometry.

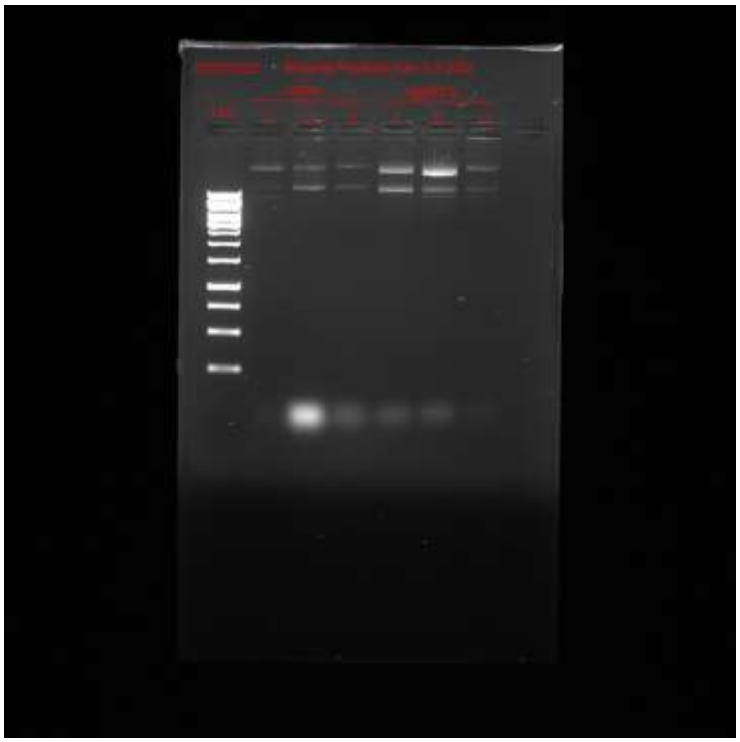

Figure 4. Agarose gel electrophoresis image of the pAAV-Ef1α-DIO eNpHR3.0-EYFP (eNpHR3.0) and the pAAV2.5-THP-GFP/WGA (WGA). 1KB indicates a GeneRuler © 1KB ladder, while 1, 2, and 3, indicate the reaction number for each alkaline miniprep performed for WGA and eNpHR3.0. Concentrations for each plasmid were recorded using a nanodrop spectrophotometer and are 1 = 4.585 $\frac{\text{ng}}{\mu L}$, 2 = 2550 $\frac{\text{ng}}{\mu L}$, and 3 = 1948 $\frac{\text{ng}}{\mu L}$ for each WGA recording and 1 = 1804 $\frac{\text{ng}}{\mu L}$, 2 = 1751 $\frac{\text{ng}}{\mu L}$, and 3 = 838.4 $\frac{\text{ng}}{\mu L}$ for each eNpHR3.0 recording.

The WGA gene was located at the 3403 bp from the ori in pAAV2.5-THP-GFP/WGA. In order to confirm that the sequence located from 3403 – 4020 bp was WGA, a nucleotide BLAST was performed on this 620 bp sequence (Figure 5). A match with WGA isolectin D was found with a paired identity of 98.83% and an E value of 0.

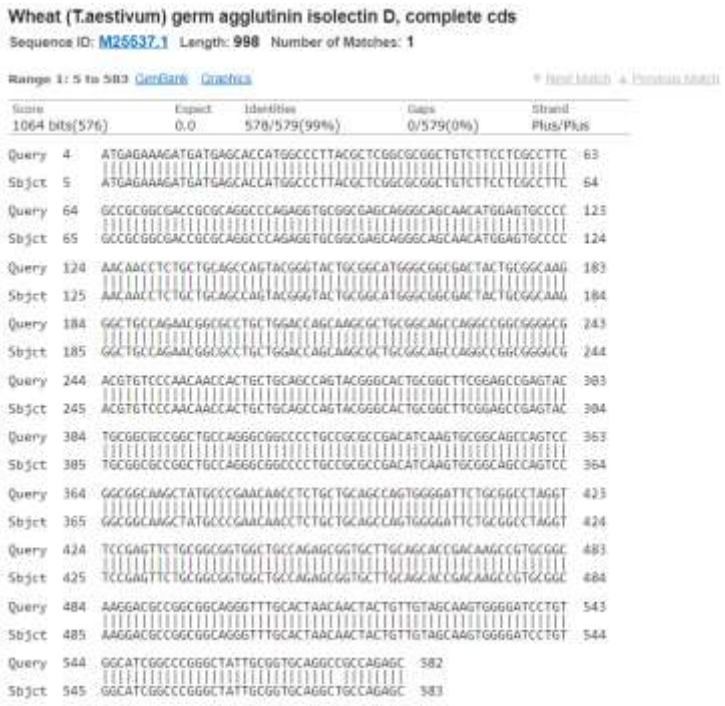

Wheat (T.aestivum) germ agglutinin isolectin D, complete cds

Sequence ID: M25637.1 Length: 998 Number of Matches: 1

Range 1: 5 to 583 GenBank Graphics

Score	Expect	Identities	Gaps	Strand
1064 bits(576)	0.0	578/579(99%)	0/579(0%)	Plus/Plus

```
Query  4    ATGAGAAAGATGATGAGCACCATGGCCCTTACGCTCGGCGCGGCTGTCTTCCTCGCCTTC  63
            ||||||||||||||||||||||||||||||||||||||||||||||||||||||||||||
Sbjct  5    ATGAGAAAGATGATGAGCACCATGGCCCTTACGCTCGGCGCGGCTGTCTTCCTCGCCTTC  64

Query  64   GCCGCGGCGACCGCGCAGGCCCAGAGGTGCGGCGAGCAGGGCAGCAACATGGAGTGCCCC  123
            ||||||||||||||||||||||||||||||||||||||||||||||||||||||||||||
Sbjct  65   GCCGCGGCGACCGCGCAGGCCCAGAGGTGCGGCGAGCAGGGCAGCAACATGGAGTGCCCC  124

Query  124  AACAACCTCTGCTGCAGCCAGTACGGGTACTGCGGCATGGGCGGCGACTACTGCGGCAAG  183
            ||||||||||||||||||||||||||||||||||||||||||||||||||||||||||||
Sbjct  125  AACAACCTCTGCTGCAGCCAGTACGGGTACTGCGGCATGGGCGGCGACTACTGCGGCAAG  184

Query  184  GGCTGCCAGAACGGCGCCTGCTGGACCAGCAAGCGCTGCGGCAGCCAGGCCGGCGGGGCG  243
            ||||||||||||||||||||||||||||||||||||||||||||||||||||||||||||
Sbjct  185  GGCTGCCAGAACGGCGCCTGCTGGACCAGCAAGCGCTGCGGCAGCCAGGCCGGCGGGGCG  244

Query  244  ACGTGTCCCAACAACCACTGCTGCAGCCAGTACGGGCACTGCGGCTTCGGAGCCGAGTAC  303
            ||||||||||||||||||||||||||||||||||||||||||||||||||||||||||||
Sbjct  245  ACGTGTCCCAACAACCACTGCTGCAGCCAGTACGGGCACTGCGGCTTCGGAGCCGAGTAC  304

Query  304  TGCGGCGCCGGCTGCCAGGGCGGCCCCTGCCGCGCCGACATCAAGTGCGGCAGCCAGTCC  363
            ||||||||||||||||||||||||||||||||||||||||||||||||||||||||||||
Sbjct  305  TGCGGCGCCGGCTGCCAGGGCGGCCCCTGCCGCGCCGACATCAAGTGCGGCAGCCAGTCC  364

Query  364  GGCGGCAAGCTATGCCCGAACAACCTCTGCTGCAGCCAGTGGGGATTCTGCGGCCTAGGT  423
            ||||||||||||||||||||||||||||||||||||||||||||||||||||||||||||
Sbjct  365  GGCGGCAAGCTATGCCCGAACAACCTCTGCTGCAGCCAGTGGGGATTCTGCGGCCTAGGT  424

Query  424  TCCGAGTTCTGCGGCGGTGGCTGCCAGAGCGGTGCTTGCAGCACCGACAAGCCGTGCGGC  483
            ||||||||||||||||||||||||||||||||||||||||||||||||||||||||||||
Sbjct  425  TCCGAGTTCTGCGGCGGTGGCTGCCAGAGCGGTGCTTGCAGCACCGACAAGCCGTGCGGC  484

Query  484  AAGGACGCCGGCGGCAGGGTTTGCACTAACAACTACTGTTGTAGCAAGTGGGGATCCTGT  543
            ||||||||||||||||||||||||||||||||||||||||||||||||||||||||||||
Sbjct  485  AAGGACGCCGGCGGCAGGGTTTGCACTAACAACTACTGTTGTAGCAAGTGGGGATCCTGT  544

Query  544  GGCATCGGCCCGGGCTATTGCGGTGCAGGCCGCCAGAGC  582
            |||||||||||||||||||||||||||||| |||||||
Sbjct  545  GGCATCGGCCCGGGCTATTGCGGTGCAGGCTGCCAGAGC  583
```

Figure 5. Nucleotide BLAST results for WGA from plasmid compared to a similar sequence of WGA-D from cDNA.

Previous work demonstrated that modification of nucleotides at the N-terminus of eNpHR3.0 did not detract from the functionality of the actuator (Gradinaru et al., 2010). Using NEBCutter V2.0 (http://nc2.neb.com/NEBcutter2/), a unique NheI restriction site within the lox sequences and at the N-terminus of eNpHR3.0 was identified as the insertion site, 3255 bp from the Ori of the pAAV-EF1α-DIO eNpHR3.0-EYFP plasmid (Figure 6). Therefore, NheI restriction enzyme sequences were added to mutagenic PCR primers in order to flank the WGA fragment with NheI sequences. A single nucleotide was added to the 5' of each restriction enzyme cut site in order to aid the binding of the NheI endonuclease. These primers are:

Forward – 5'-G<u>GCTAGC</u>TCCGGCCGGACTC-3' (annealing temp = 71.7 °C)

Reverse – 5'-C<u>GCTAGC</u>TTAAGCGTCACAGCCGCC-3' (annealing temp = 73.9 °C)

The NheI binding sequence is underlined. A primer dimer calculating software was used from Thermofisher, and minimal primer dimers were found to be present with these two primer sequences. Annealing temperatures were also calculated using a Thermofisher primer calculator tool, thus a temperature of 71.7 °C was used for the annealing phase of the PCR.

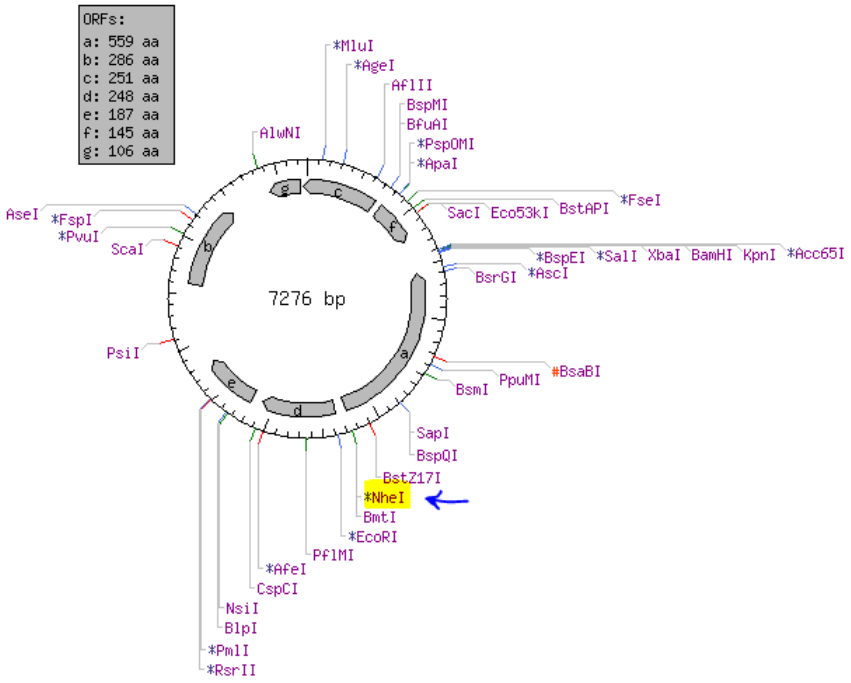

Figure 6. NheI restriction site on pAAV-Ef1α-DIO eNpHR3.0-EYFP

After performing a PCR on pAAV2.5-THP-GFP/WGA with mutagenic primers at an annealing temperature of 71.7 ˚C, it was anticipated that the PCR product would be approximately 620 bp long, the length of the WGA gene. This was verified using an agarose gel electrophoresis of the PCR product (Figure 7). However, additional bands can be seen. Since this degree of amplification non-specificity would negatively impact the ligation process, and performing a gel extraction procedure to extract the correct PCR product would only decrease the yield, the PCR reaction was performed again but with an annealing temperature of 72.4˚C. These subsequent PCR reactions produced single bands at the target length and can be seen post restriction digest in Figure 8.

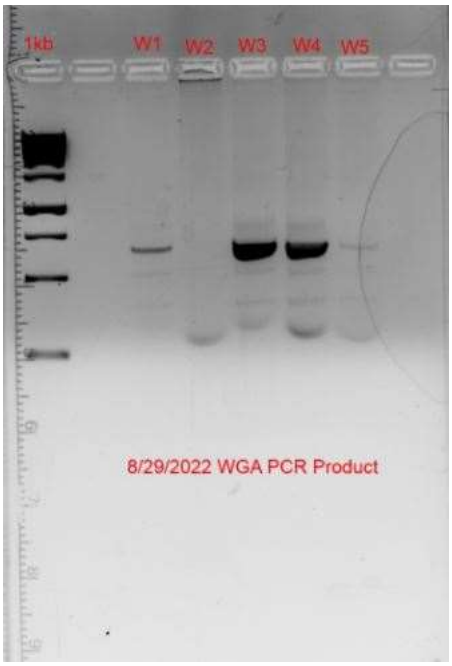

Figure 7. Gel electrophoresis of the mutagenic PCR

It was necessary to digest both the eNpHR3.0 plasmid and the WGA PCR product with NheI restriction endonucleases in order to insert the WGA gene into the eNpHR3.0 plasmid.

Figure 8. NheI digests of eNpHR3.0 and WGA PCR product

Following successful digestion (confirmed via agarose electrophoresis) and removal of the restriction enzyme by phenol:chloroform extraction, T4 ligation reactions were prepared on two preparations of PCR product and vector insert DNA, each having vector to insert ratios of 1:1, 1:3, 1:6, and 1:12. The first preparation included WGA and eNpHR3.0 DNA both digested with NheI restriction endonuclease, while the second preparation did not digest the WGA PCR

fragment and instead blunted the 5' overhang on the NheI cleavage site in eNpHR3.0 with a DNA Polymerase I, Large Klenow Fragment. Ligation reactions were incubated at 16 °C overnight and reaction samples were then transformed into Stbl3 UCCs with ampicillin selection (20 $\frac{\mu g}{mL}$) on LB agar. Minicultures were prepared and plasmids were extracted by alkaline lysis miniprep. Potential clones were classified as sticky end or blunt end in an agarose electrophoresis (Figure 9). Isolated plasmids from these cells were then verified to contain successful inserts of WGA by comparing eNpHR3.0 plasmids to WGA→eNpHR3.0 plasmids, where the latter would be 620 bp longer than the former. Samples that showed positive results were sent to IDTDNA for sequencing.

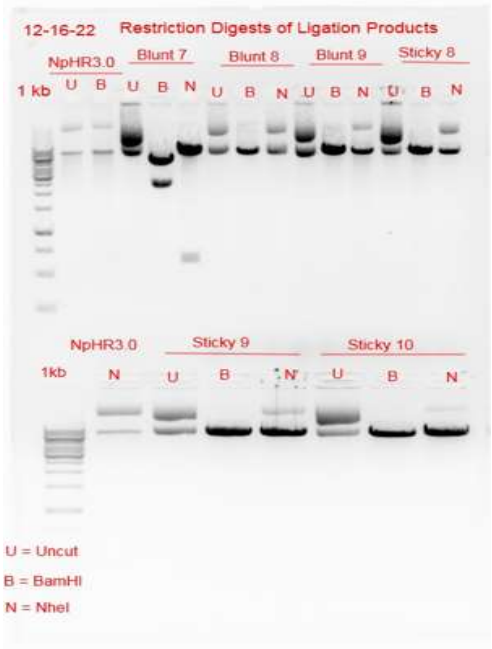

Figure 9. Electrophoresis gel results of WGA→eNpHR3.0. The top of the gel represents minipreps of sticky-end ligation reactions. The bottom of the gel represents minipreps of blunt-end ligations.

DISCUSSION

This thesis demonstrates the creation of a transsynaptic halorhodopsin where the WGA peptide was successfully fused to the N-terminus of eNpHR3.0-EYFP. The WGA sequence was amplified by PCR and ligated just upstream of the N-terminus of eNpHR3.0 on pAAV-Ef1α-DIO EYFP-eNpHR3.0. Our novel WGA-eNpHR3.0 provides an innovative tool for retrograde transsynaptic trafficking of an optogenetic actuator to afferent neurons for *in vivo* and *in vitro* dissection of neural circuits.

Before *in vivo* application of this construct, *in vitro* tests will be performed to confirm trafficking and to test the functional efficacy of WGA-eNpHR3.0. To test for translocation of the WGA-eNpHR3.0-EYFP construct, co-cultures of Cre-positive and Cre-negative neurons will be prepared and infected with AAV_WGA-eNpH3.0-EYFP or AAV_eNpHR3.0-EYFP. Immunohistochemistry and confocal microscopy will be performed on these cultures. Primary antibodies targeting Cre recombinase (with a red secondary antibody) and eNpHR3.0 (with a green secondary antibody) will be co-applied. We expect that infection with AAV_eNpH3.0-EYFP will produce an eNpHR3.0 (and EYFP) signal only in Cre-positive neurons. In contrast, we predict that infection with AAV_WGA-eNpHR3.0-EYFP will produce eNpHR3.0 (and EYFP) signal in Cre-positive and Cre-negative neurons due to transsynaptic movement of the construct. It is possible to also patch clamp record and depolarize the neurons during illumination of the culture. If eNpHR3.0 is present at sufficient levels, it should be possible to prevent depolarization induced action potential discharge in the Cre-negative neurons. To further test function, PV-Cre mice will be infected in area CA1 with AAV_WGA-eNpHR3.0-EYFP. One week later,

hippocampal slices will be prepared, and stimulated electrodes will be placed to activate either CA3 or EC afferents. We will then patch clamp record from PV+ interneurons and apply electrical stimulation with or without co-activation of eNpHR3.0. We expect electrical stimulation to induce excitatory postsynaptic currents in PV+ interneurons in the absence of eNpHR3.0 illumination and reduced or no synaptic currents during eNpHR3.0 illumination.

Following these basic tests of function, we propose to use this construct to infect PV+ interneurons in area CA1 of the rat hippocampus to selectively inhibit excitatory afferents arriving from area CA3 or the entorhinal cortex during execution of a goal-directed spatial learning and memory task (Figure 10). We predict that the illumination of area CA3 will selectively inhibit slow gamma and illumination of the EC will selectively inhibit fast gamma. We further predict that illumination of area CA3, but not the EC, only while the animal is immobile at the start of memory probe trials will impair goal location recall. In contrast, we predict that illumination of the EC, but not area CA3, while the animal is moving will impair navigation to the goal location. If these predictions hold, we will have definitively described how network oscillations in CA1 regulate the cognitive state of the animal with respect to its ability to retrieve a goal location from long-term memory and to execute efficient paths to remembered goal locations.

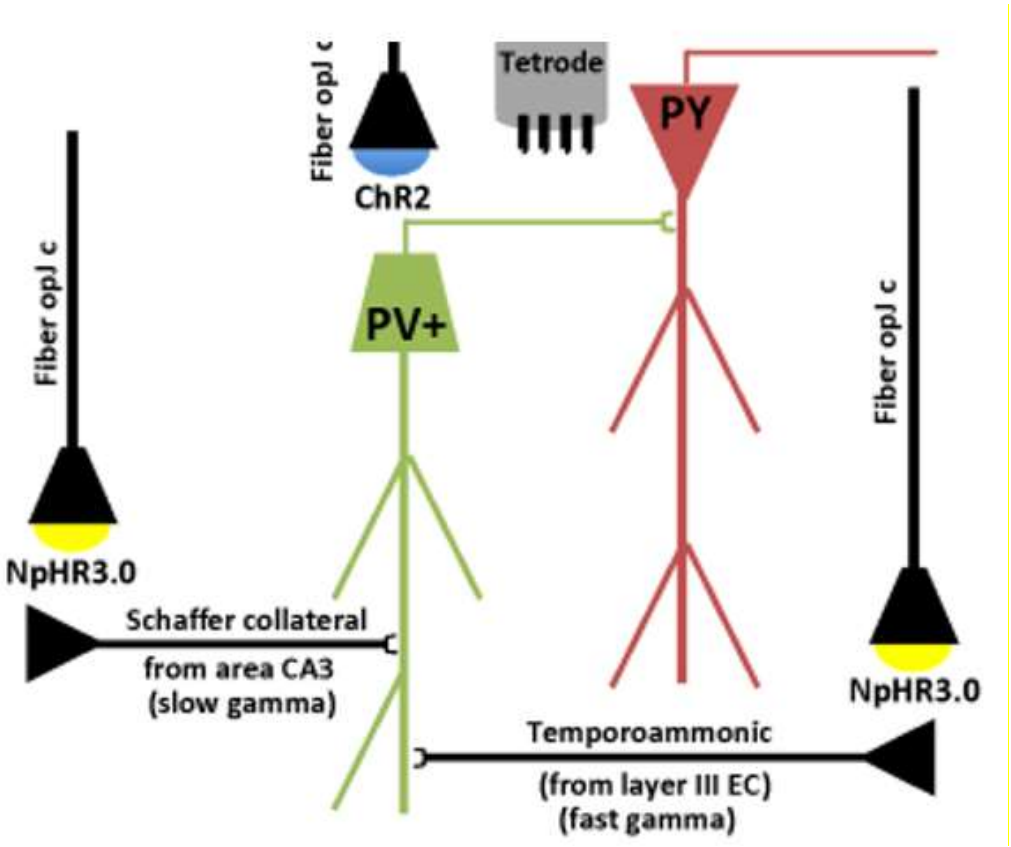

Figure 10. Area CA1 network under investigation. Diagram shows a pyramidal cell (PY) and a PV-positive FSI (PV+) with afferents from area CA3 and layer III of the EC. ChR2 is expressed in the PV-positive FSIs. NpHR3.0 is expressed in the afferent cells.

If our WGA-eNpHR3.0 construct is capable of transsynaptic trafficking, there are additional hurdles that would need to be overcome. There is likelihood of expression of WGA-eNpHR3.0 in both the originally transfected neuron as well as the trafficked afferent neuron and a possibility of disynaptic trafficking to afferents of the afferent neurons upstream of the ROI. The former issue is minimal due to the ability to restrict activation to area CA3 or the entorhinal cortex. The latter issue will be investigated with immunohistochemistry. Another potential drawback to this approach would be the possibility of a bottleneck in trafficking, limiting the

number of constructs that are able to be expressed in afferent neurons. This obstacle may be overcome through a high throughput directed evolution approached via error-prone PCR techniques that selectively evolve constructs that traffic a sufficient concentration of WGA-eNpHR3.0 proteins from neuron to its afferent.

When considering the effect that a trafficking bottleneck could potentially have on the efficacy of the construct, a physiologically functional amount of eNpHR3.0 expression can be calculated *a priori*. The current version of eNpHR3.0 has been empirically measured in Xenopus Laevis oocytes and is recorded to transport approximately 219 (+/- 98) chloride ions/protein/s across the membrane, thus converting to amperes by multiplying the number of chloride ions/protein/s by the charge of chloride gives $3.5084\text{x}10^{-5}$ pA (Feroz et al., 2018). Combining this information with records of a peak current of approximately 62 pA being capable of silencing a pyramidal neuron with 594 nm, 5 mW light, a calculation can be performed to generate the total number of halorhodopsins necessary to silence a neuron under physiological conditions, which is approximately $1.767x10^{6}$ proteins/neuron (Zhang et al., 2019). In contrast, optogenetic inhibitors that are ion channels may require less expression yields and may not be affected by a trafficking bottleneck to the extent that halorhodopsin might be. This is because ion channels are not dependent upon an isomerization for each ion transported across the membrane.

As described above, protein-based trafficking strategies may suffer from limitations due to the quantity of construct that is required for full functionality. Alternatively, there exist viral-based strategies that transmit genetic material and are capable of transfecting projection neurons by entering their axons and trafficking to their soma (Tervo et al., 2016). Such viruses include rabies viruses, but perhaps more relevant, rAAV2-retro. rAAV2-retro is the most promising approach for retrograde trafficking of transgene constructs to afferent neurons as it is capable of transfecting an afferent neuron with a minimal aliquot of virus. A downside to this is a relative

lack of cellular specificity since transformation is based on spatial reach of the injected virus. This specificity problem can be partially overcome with incorporation of cell specific promoters. For instance, rAAV2-retro may be combined with WGA-eNpHR3.0 to efficiently transfect afferent neurons in a general vicinity and limit expression of WGA-eNpHR3.0 to target cell populations through genetically defined promoters with trafficking to the neuronal soma facilitated by WGA.

In summary, WGA represents an interesting approach to trafficking optogenetic constructs retrogradely and transynaptically. Since modern functional dissection of neural circuits now involve optogenetics, optimizing tools for cell-specific protein trafficking holds tremendous promise.

REFERENCES

Arnolds, D. E. A. T., Lopes Da Silva, F. H., Aitink, J. W., Kamp, A., & Boeijinga, P. (1980). The spectral properties of hippocampal EEG related to behavior in man. *Electroencephalography and Clinical Neurophysiology*, *50*(3-4), 324–328. https://doi.org/10.1016/0013-4694(80)90160-1

Ash, C., Dubec, M., Donne, K., & Bashford, T. (2017). Effect of wavelength and beam width on penetration in light-tissue interaction using computational methods. *Lasers in Medical Science*, *32*(8), 1909–1918. https://doi.org/10.1007/s10103-017-2317-4

Baker, H., & Spencer, R. F. (1986). Transneuronal transport of peroxidase-conjugated wheat germ agglutinin (WGA-HRP) from the olfactory epithelium to the brain of the adult rat. *Experimental Brain Research*, *63*(3), 461–473. https://doi.org/10.1007/bf00237470

Belluscio MA, Mizuseki K, Schmidt R, Kempter R, Buzsáki G (2012) Cross-frequency phase-phase coupling between θ and γ oscillations in the hippocampus. J Neurosci 32(2):423-35. PMID:22238079

Bragin, A., Jando, G., Nadasdy, Z., Hetke, J., Wise, K., & Buzsaki, G. (1995). Gamma (40-100 Hz) oscillation in the hippocampus of the behaving rat. *The Journal of Neuroscience*, *15*(1), 47–60. https://doi.org/10.1523/jneurosci.15-01-00047.1995

Broadwell, R. D., & Balin, B. J. (1985). Endocytic and exocytic pathways of the neuronal secretory process and trans synaptic transfer of wheat germ agglutinin-horseradish peroxidasein vivo. *The Journal of Comparative Neurology*, *242*(4), 632–650. https://doi.org/10.1002/cne.902420410

Brun VH, Otnass MK, Molden S, Steffenach HA, Witter MP, Moser MB, Moser EI (2002) Place cells and place recognition maintained by direct entorhinal-hippocampal circuitry. Science 296(5576):2243-6. PMID:12077421

Buzsáki G (2015) Hippocampal sharp wave-ripple: A cognitive biomarker for episodic memory and planning. Hippocampus 25(10):1073-188. PMID:26135716

Buzsáki, G. (2005). Theta rhythm of navigation: Link between Path Integration and landmark navigation, episodic and semantic memory. *Hippocampus*, *15*(7), 827–840. https://doi.org/10.1002/hipo.20113

Cabral HO, Vinck M, Fouquet C, Pennartz CM, Rondi-Reig L, Battaglia FP (2014) Oscillatory dynamics and place field maps reflect hippocampal ensemble processing of sequence and place memory under NMDA receptor control. Neuron 81:402-15. PMID:24462101

Callaway, E. M., & Luo, L. (2015). Monosynaptic circuit tracing with glycoprotein-deleted rabies viruses. *Journal of Neuroscience*, *35*(24), 8979–8985. https://doi.org/10.1523/jneurosci.0409-15.2015

Colgin LL (2016) Rhythms of the hippocampal network. Nat Rev Neurosci 17(4):239-49. PMID:26961163

Colgin LL, Denninger T, Fyhn M, Hafting T, Bonnevie T, Jensen O, Moser MB, Moser EI (2009) Frequency of gamma oscillations routes flow of information in the hippocampus. Nature 462(7271):353-7. PMID:19924214

Colgin, L. L., & Moser, E. I. (2010). Gamma oscillations in the hippocampus. *Physiology*, *25*(5), 319–329. https://doi.org/10.1152/physiol.00021.2010

Damak, S., Mosinger, B., & Margolskee, R. F. (2008). Transsynaptic transport of wheat germ agglutinin expressed in a subset of type II taste cells of transgenic mice. *BMC Neuroscience*, *9*(1). https://doi.org/10.1186/1471-2202-9-96

De La Crompe, B., Coulon, P., & Diester, I. (2020). Functional interrogation of neural circuits with virally transmitted optogenetic tools. *Journal of Neuroscience Methods*, *345*, 108905. https://doi.org/10.1016/j.jneumeth.2020.108905

Deshmukh, S. S., Yoganarasimha, D., Voicu, H., & Knierim, J. J. (2010). Theta modulation in the medial and the lateral entorhinal cortices. *Journal of Neurophysiology*, *104*(2), 994–1006. https://doi.org/10.1152/jn.01141.2009

Diba K, Buzsáki G (2007) Forward and reverse hippocampal place-cell sequences during ripples. Nat Neurosci 10(10):1241-2. PMID:17828259

Feroz, H. M. (2017). Measuring transport kinetics of light driven chloride pump, Halorhodopsin. *Biophysical Journal*, *112*(3). https://doi.org/10.1016/j.bpj.2016.11.3075

Fyhn M, Molden S, Witter MP, Moser EI, Moser MB (2004) Spatial representation in the entorhinal cortex. Science 305(5688):1258-64. PMID:15333832

Gentet, L. J., Stuart, G. J., & Clements, J. D. (2000). Direct measurement of specific membrane capacitance in neurons. *Biophysical Journal*, *79*(1), 314–320. https://doi.org/10.1016/s0006-3495(00)76293-x

Gradinaru, V., Zhang, F., Ramakrishnan, C., Mattis, J., Prakash, R., Diester, I., Goshen, I., Thompson, K. R., & Deisseroth, K. (2010). Molecular and cellular approaches for diversifying and extending optogenetics. *Cell*, *141*(1), 154–165. https://doi.org/10.1016/j.cell.2010.02.037

Grastyán, E., Lissák, K., Madarász, I., & Donhoffer, H. (1959). Hippocampal electrical activity during the development of conditioned reflexes. *Electroencephalography and Clinical Neurophysiology*, *11*(3), 409–430. https://doi.org/10.1016/0013-4694(59)90040-9

Grosenick, L., Marshel, J. H., & Deisseroth, K. (2015). Closed-Loop and activity-guided OPTOGENETIC CONTROL. *Neuron*, *86*(1), 106–139. https://doi.org/10.1016/j.neuron.2015.03.034

Guru, A., Post, R. J., Ho, Y.-Y., & Warden, M. R. (2015). Making sense of optogenetics. *International Journal of Neuropsychopharmacology*, *18*(11). https://doi.org/10.1093/ijnp/pyv079

Hafting T, Fyhn M, Molden S, Moser MB, Moser EI (2005) Microstructure of a spatial map in the entorhinal cortex. Nature 436(7052):801-6. PMID:15965463

Hasselmo ME, Stern CE (2014) Theta rhythm and the encoding and retrieval of space and time. Neuroimage 85 Pt 2(02):656-66. PMID:23774394

Headley DB, Paré D (2017) Common oscillatory mechanisms across multiple memory systems. NPJ Sci Learn 2:1. PMID:30294452Jazayeri, M., & Afraz, A. (2017). Navigating the neural space in search of the neural code. *Neuron*, *93*(5), 1003–1014. https://doi.org/10.1016/j.neuron.2017.02.019

Jazayeri, M., & Afraz, A. (2017). Navigating the neural space in search of the neural code. *Neuron*, *93*(5), 1003–1014. https://doi.org/10.1016/j.neuron.2017.02.019

Johnson A, Redish AD (2007) Neural ensembles in CA3 transiently encode paths forward of the animal at a decision point. J Neurosci 27(45):12176-89. PMID:17989284

Kato, H. E., Kim, Y. S., Paggi, J. M., Evans, K. E., Allen, W. E., Richardson, C., Inoue, K., Ito, S., Ramakrishnan, C., Fenno, L. E., Yamashita, K., Hilger, D., Lee, S. Y. Berndt, A., Shen, K., Kandori, H., Dror, R. O., Kobilka, B. K., & Deisseroth, K. (2018). Structural mechanisms of selectivity and gating in anion channelrhodopsins. *Nature*, *561*(7723), 349–354.

https://doi.org/10.1038/s41586-018-0504-5
Kim, C. K., Adhikari, A., & Deisseroth, K. (2017). Integration of optogenetics with complementary methodologies in systems neuroscience. *Nature Reviews Neuroscience*, *18*(4), 222–235. https://doi.org/10.1038/nrn.2017.15
Kimble, D. P. (1963). The effects of bilateral hippocampal lesions in rats. *Journal of Comparative and Physiological Psychology*, *56*(2), 273–283. https://doi.org/10.1037/h0048903
Kwon, I., & Schaffer, D. V. (2007). Designer gene delivery vectors: Molecular Engineering and evolution of adeno-associated viral vectors for enhanced gene transfer. *Pharmaceutical Research*, *25*(3). https://doi.org/10.1007/s11095-007-9431-0
Lin, D., Boyle, M. P., Dollar, P., Lee, H., Lein, E. S., Perona, P., & Anderson, D. J. (2011). Functional identification of an aggression locus in the mouse hypothalamus. *Nature*, *470*(7333), 221–226. https://doi.org/10.1038/nature09736
Luo, L., Callaway, E. M., & Svoboda, K. (2008). Genetic dissection of neural circuits. *Neuron*, *57*(5), 634–660. https://doi.org/10.1016/j.neuron.2008.01.002
Maguire, E. A., Nannery, R., & Spiers, H. J. (2006). Navigation around London by a taxi driver with bilateral hippocampal lesions. *Brain*, *129*(11), 2894–2907. https://doi.org/10.1093/brain/awl286
Mattis, J., Tye, K. M., Ferenczi, E. A., Ramakrishnan, C., O'Shea, D. J., Prakash, R., Gunaydin, L. A., Hyun, M., Fenno, L. E., Gradinaru, V., Yizhar, O., & Deisseroth, K. (2011). Principles for applying optogenetic tools derived from direct comparative analysis of microbial opsins. *Nature Methods*, *9*(2), 159–172. https://doi.org/10.1038/nmeth.1808
McCarty, D. M., Monahan, P. E., & Samulski, R. J. (2001). Self-complementary recombinant adeno-associated virus (scaav) vectors promote efficient transduction independently of DNA synthesis. *Gene Therapy*, *8*(16), 1248–1254. https://doi.org/10.1038/sj.gt.3301514
Mitchell, S. J., & Ranck, J. B. (1980). Generation of theta rhythm in medial entorhinal cortex of freely moving rats. *Brain Research*, *189*(1), 49–66. https://doi.org/10.1016/0006-8993(80)90006-2
Nagel, G., Szellas, T., Huhn, W., Kateriya, S., Adeishvili, N., Berthold, P., Ollig, D., Hegemann, P., & Bamberg, E. (2003). Channelrhodopsin-2, a directly light-gated cation-selective membrane channel. *Proceedings of the National Academy of Sciences*, *100*(24), 13940–13945. https://doi.org/10.1073/pnas.1936192100
Oesterhelt, D., Hegemann, P., & Tittor, J. (1985). The photocycle of the chloride pump halorhodopsin. II: Quantum yields and a kinetic model. *The EMBO Journal*, *4*(9), 2351–2356. https://doi.org/10.1002/j.1460-2075.1985.tb03938.x
O'Keefe, J., & Nadel, L. (1978). *The hippocampus as a cognitive map*. Clarendon Press.
O'Keefe, J., & Dostrovsky, J. (1971). The hippocampus as a spatial map. Preliminary evidence from unit activity in the freely-moving rat. *Brain Research*, *34*(1), 171–175. https://doi.org/10.1016/0006-8993(71)90358-1
O'Keefe, J., & Recce, M. L. (1993). Phase relationship between hippocampal place units and the EEG theta rhythm. *Hippocampus*, *3*(3), 317–330. https://doi.org/10.1002/hipo.450030307
Osakada, F., Mori, T., Cetin, A. H., Marshel, J. H., Virgen, B., & Callaway, E. M. (2012). New rabies virus variants for monitoring and manipulating activity and gene expression in defined neural circuits. *Neuron*, *74*(1), 206. https://doi.org/10.1016/j.neuron.2012.03.019
Pfeiffer BE, Foster DJ (2013) Hippocampal place-cell sequences depict future paths to remembered goals. Nature 497(7447):74-9. PMID:23594744
Robinson, N. T. M., Descamps, L. A. L., Russell, L. E., Buchholz, M. O., Bicknell, B. A., Antonov, G. K., … Häusser, M. (2020). Targeted Activation of Hippocampal Place Cells

Drives Memory-Guided Spatial Behavior. *Cell*, *183*(7), 2041–2042. https://doi.org/10.1016/j.cell.2020.12.010
Raimondo, J. V., Kay, L., Ellender, T. J., & Akerman, C. J. (2012). Optogenetic silencing strategies differ in their effects on inhibitory synaptic transmission. *Nature Neuroscience*, *15*(8), 1102–1104. https://doi.org/10.1038/nn.3143
Sakaguchi, T., Ishikawa, D., Nomura, H., Matsuki, N., & Ikegaya, Y. (2012). Normal learning ability of mice with a surgically exposed hippocampus. *NeuroReport*, *23*(7), 457–461. https://doi.org/10.1097/wnr.0b013e32835375b6
Shipley, M. T. (1985). Transport of molecules from nose to brain: Transneuronal anterograde and retrograde labeling in the rat olfactory system by wheat germ agglutinin-horseradish peroxidase applied to the nasal epithelium. *Brain Research Bulletin*, *15*(2), 129–142. https://doi.org/10.1016/0361-9230(85)90129-7
Schwab, M. E., Javoy-Agid, F., & Agid, Y. (1978). Labeled Wheat Germ agglutinin (WGA) as a new, highly sensitive retrograde tracer in the rat brain hippocampal system. *Brain Research*, *152*(1), 145–150. https://doi.org/10.1016/0006-8993(78)90140-3
Senior TJ, Huxter JR, Allen K, O'Neill J, Csicsvari J (2008) Gamma oscillatory firing reveals distinct populations of pyramidal cells in the CA1 region of the hippocampus. J Neurosci 28(9):2274-86. PMID:18305260
Steffenach HA, Sloviter RS, Moser EI, Moser MB (2002) Impaired retention of spatial memory after transection of longitudinally oriented axons of hippocampal CA3 pyramidal cells. Proc Natl Acad Sci USA 99(5):3194-8. PMID:11867718
Stumpf, C., Petsche, H., & Gogolak, G. (1962). The significance of the rabbit's septum as a relay station between the midbrain and the hippocampus II. The differential influence of drugs upon both the septal cell firing pattern and the hippocampus theta activity. *Electroencephalography and Clinical Neurophysiology*, *14*(2), 212–219. https://doi.org/10.1016/0013-4694(62)90031-7
Suzuki, T., Morimoto, N., Akaike, A., & Osakada, F. (2020). Multiplex Neural Circuit tracing with G-deleted rabies viral vectors. *Frontiers in Neural Circuits*, *13*. https://doi.org/10.3389/fncir.2019.00077
Taube, J. S., Muller, R. U., & Ranck, J. B. (1990). Head-direction cells recorded from the postsubiculum in freely moving rats. I. Description and quantitative analysis. *The Journal of Neuroscience*, *10*(2), 420–435. https://doi.org/10.1523/jneurosci.10-02-00420.1990
Tervo, D. G. R., Hwang, B.-Y., Viswanathan, S., Gaj, T., Lavzin, M., Ritola, K. D., Lindo, S., Michael, S., Kuleshova, E., Ojala, D., Huang, C.-C., Gerfen, C. R., Schiller, J., Dudman, J. T., Hantman, A. W., Looger, L. L., Schaffer, D. V., & Karpova, A. Y. (2016). A designer AAV variant permits efficient retrograde access to projection neurons. *Neuron*, *92*(2), 372–382. https://doi.org/10.1016/j.neuron.2016.09.021
Wickersham, I. R., Lyon, D. C., Barnard, R. J. O., Mori, T., Finke, S., Conzelmann, K.-K., Young, J. A. T., & Callaway, E. M. (2007). Monosynaptic restriction of transsynaptic tracing from single, genetically targeted neurons. *Neuron*, *53*(5), 639–647. https://doi.org/10.1016/j.neuron.2007.01.033
Wiegert, J. S., Mahn, M., Prigge, M., Printz, Y., & Yizhar, O. (2017). Silencing neurons: Tools, applications, and experimental constraints. *Neuron*, *95*(3), 504–529. https://doi.org/10.1016/j.neuron.2017.06.050
Wietek, J., Beltramo, R., Scanziani, M., Hegemann, P., Oertner, T. G., & Wiegert, J. S. (2015). An improved chloride-conducting channelrhodopsin for light-induced inhibition of neuronal activity in vivo. *Scientific Reports*, *5*(1). https://doi.org/10.1038/srep14807
Wikenheiser, A. M., & Redish, A. D. (2015). Hippocampal theta sequences reflect current goals.

Nature Neuroscience, *18*(2), 289–294. https://doi.org/10.1038/nn.3909

Yoshihara, Y., Mizuno, T., Nakahira, M., Kawasaki, M., Watanabe, Y., Kagamiyama, H., Jishage, K.-ichi, Ueda, O., Suzuki, H., Tabuchi, K., Sawamoto, K., Okano, H., Noda, T., & Mori, K. (1999). A genetic approach to visualization of multisynaptic neural pathways using plant lectin transgene. *Neuron*, *22*(1), 33–41. https://doi.org/10.1016/s0896-6273(00)80676-5

Zhang, C., Yang, S., Flossmann, T., Gao, S., Witte, O. W., Nagel, G., Holthoff, K., & Kirmse, K. (2019). Optimized photo-stimulation of halorhodopsin for long-term neuronal inhibition. *BMC Biology*, *17*(1). https://doi.org/10.1186/s12915-019-0717-6

Zheng C, Bieri KW, Trettel SG, Colgin LL (2015) The relationship between gamma frequency and running speed differs for slow and fast gamma rhythms in freely behaving rats. Hippocampus 25(8):924-38. PMID:25601003

BIOGRAPHY

Lucas Kinsey earned his Bachelor of Science in the year 2020 and immediately sought to earn a Master of Science degree while working as a student researcher in Dr. Theodore Dumas's lab. Lucas is also employed in Dr. Karel Svoboda's lab as a research associate training mice to perform decision-making tasks where he is learning the applications of optical physiology.